Neurosci Bull August 1, 2010, 26(4): 289-296. http://www.neurosci.cn
DOI: 10.1007/s12264-010-0122-1

·Original Article·

Pharmacological modulation of brain Nav1.2 and cardiac Nav1.5 subtypes by the local anesthetic ropivacaine

Hui-Wen CHENG*, Hong-Tian YANG*, Jing-Jing ZHOU, Yong-Hua JI, Hong-Yan ZHU

Laboratory of Neuropharmacology and Neurotoxicology, Shanghai University, Shanghai 200444, China

Abstract: Objective The present study was aimed to investigate the pharmacological modulatory effects of ropivacaine, an amide-type local anesthetic, on rat Nav1.2 (rNav1.2) and rNav1.5, the two Na^+ channel isoforms heterologously expressed in *Xenopus* oocytes and in HEK293t cell line, respectively. **Methods** Two-electrode voltage-clamp (TEVC) and whole-cell patch-clamp recordings were employed to record the whole-cell currents. **Results** Ropivacaine induced tonic inhibition of peak Na^+ currents of both subtypes in a dose- and frequency-dependent manner. rNav1.5 appeared to be more sensitive to ropivacaine. In addition, for both Na^+ channel subtypes, the steady-state inactivation curves, but not the activation curves, were significantly shifted to the hyperpolarizing direction by ropivacaine. Use-dependent blockade of both rNav1.2 and rNav1.5 channels was induced by ropivacaine through a high frequency of depolarization, suggesting that ropivacaine could preferentially bind to the 2 inactivated Na^+ channel isoforms. **Conclusion** The results will be helpful in understanding the pharmacological modulation by ropivacaine on Nav1.2 subtype in the central nervous system, and on Nav1.5 subtype abundantly expressed in the heart.

Keywords: ropivacaine; local anesthetic drug; Na^+ channel subtype-sensitivity; electrophysiological recording

1 Introduction

1-Propyl-2', 6'-pipecoloxylidide (ropivacaine) is an amide-type local anesthetic that shares a similar structure with bupivacaine. It was initially marketed to have similar therapeutic properties with those of bupivacaine, with a long-lasting effect and less toxicity, due to its lower lipid solubility[1]. Ropivacaine is usually indicated for local anesthesia including infiltration, nerve block, epidural and intrathecal anaesthesia in adults and children over 12 years. As S(-) enantiomer has affinity for neuronal Na^+ channels comparable with R(+) enantiomer, the S(-) enantiomer of ropivacaine was prepared[2, 3].

Voltage-gated sodium channels (VGSCs) have been demonstrated to be general targets for local anesthetics by several lines of evidence[4,5]. The local anesthetics can reversibly block VGSCs in the cellular membrane of nerve cells, which prevents initiation and propagation of the nervous impulses[6]. VGSCs are transmembrane proteins consisting of a pore-forming α subunit and auxiliary β1-β4 subunits, responsible for the initial rising phase of the action potential in electrically excitable cells[7,8]. At least 10 sodium channel subtypes have been demonstrated to be selectively expressed in different tissues and cells[9,10]. Among them, Nav1.2 and Nav 1.5 are the primary isoforms expressed in the brain and in

*These authors contributed equally to this work.
Corresponding authors: Hong-Yan ZHU, Yong-Hua JI
Tel & Fax: +86-21-66135189
E-mail: zhyred@ shu.edu.cn; yhji@staff.shu.edu.cn
Article ID: 1673-7067(2010)04-0289-08
Received date: 2010-01-22; Accepted date: 2010-05-05

the heart, respectively.

Although ropivacaine has been investigated to be capable of blocking tetrodotoxin-sensitive (TTX-S) and -resistant (TTX-R) Na^+ channels in rat dorsal root ganglion (DRG) neurons[13] and Na^+ currents in the guinea pig ventricular myocytes[14], the pharmacological effect of ropivacaine on individual isoform of Na^+ channels still remains elusive. Other local anesthetics, such as lidocaine, mexiletine and benzocaine, have been confirmed to be capable of blocking rat Nav1.2α subunit (rNav1.2α) [15]. Therefore, in the present study, the sensitivities of rNav1.2α (brain type) and rNav1.5α (cardiac type) to ropivacaine, and the modulatory effects of ropivacaine on the 2 types of channels were examined, to further understand the pharmacological mechanism of ropivacaine.

2 Materials and methods

2.1 Expression of rNav1.2 and electrophysiological recording Plasmid pNa200 containing cDNA of rat brain rNav1.2α was a generous gift from Dr. Alan L. Goldin (University of California, Irvine, CA, USA) and was sequenced before RNA transcription. The cRNA of rNav1.2α was synthesized from linearized plasmid DNA (cut at Not I site) using a T7 RNA polymerase message machine transcription kit (Ambion, Inc., Austin, TX, USA). The produced cRNA was estimated by agarose gel analysis, purified, and preserved in independent ampoules at -20 °C.

Adult female X. laevis frogs were housed in a tank with constantly filtered and recirculated water maintained at 20 °C. Stage V and VI oocytes were surgically removed and treated with collagenase (2 mg/mL, type IA, Sigma), followed by agitation for 4 h in calcium-free OR2 medium with 96 mmol/L NaCl, 2 mmol/L KCl, 1 mmol/L $MgCl_2$, and 5 mmol/L HEPES (pH=7.5) at 20 °C. After being washed, healthy oocytes were selected for cRNA injection. Each oocyte was injected with 10 ng cRNA of rNav1.2α (40 nL 0.25 ng/nL cRNA solution) and then incubated in OR2 medium at 20 °C for 40 h. Other healthy oocytes were injected with 40 nL DEPC-treated water (sham injection) as a control.

The whole-cell currents were recorded by two-electrode voltage-clamp (TEC) recordings with TURBO TEC-03X amplifier (npi Instruments, Germany). Stimulation and data acquisition were conducted with Cellwork E 5.5 software (npi Instruments, Germany). A single oocyte was impaled by 2 microelectrodes filled with 3 mol/L KCl (0.2-0.7 MΩ, 1.0-2.0 MΩ, respectively) linked to the detectors with Ag/AgCl electrodes, and balanced in bath solution (ND96) for at least 30 min before recording. The electrophysiological experiments were performed at room temperature (20-25 °C). Data were collected after analog filtering at 13 kHz in voltage-clamp recording.

2.2 Expression of rNav1.5 and electrophysiological recording HEK293t cells were cultured in Dulbecco's Modified Eagle Medium (GIBCO BRL) supplemented with 10% fetal bovine serum, in an incubator with 5% CO_2. Cells were transfected with plasmids coding rNav1.5α, the α subunit of rat cardiac sodium channel (a generous gift from Dr. Kaoru Yamaoka, Hiroshima International University, Higashi-Hiroshima, Hiroshima , Japan) by using Lipofectamine 2000 (Invitrogen, USA) reagent according to the manufacturer's instructions. Briefly, one day before transfection, HEK293t cells were transferred to the 24-well plates. When reaching a confluence of 90%, cells were incubated with Lipofectamine 2000 (at a ratio of 2 μL reagent: 1 μg total plasmid per well) at 37 °C for 5-8 h. Then the medium was replaced by normal culture medium, followed by incubation for 36-48 h preceding the electrophysiological recordings. Cells with inward currents were regarded as transfection-positive ones.

Whole-cell patch-clamp recordings were conducted at room temperature using an Axopatch-200 B amplifier (Axon Instruments Inc., Union City, CA, USA). Electrophysiological recordings started 10 min after the establishment of a whole-cell configuration. To eliminate the effect of steady-state inactivation during experiments, the holding potential was set to -140 mV. The series resistance was compensated (70–80%) to minimize voltage errors. Leak subtraction was performed using a P/4 protocol before the test protocol for all voltage clamp recordings. Signals were low-pass filtered at 5 kHz and digitized at 20 kHz. Patch pipettes that had a resistance of 2-3 MΩ were used and filled with the pipette solution containing (mmol/L): CsF 140, CsCl 10, $MgCl_2$ 1, EGTA 2, and HEPES 10 (pH = 7.3). The bath solution contained (mmol/L):

NaCl 140, $MgCl_2$ 1, $CaCl_2$ 2, and HEPES 10 (pH = 7.3).

2.3 Ropivacaine application Ropivacaine (Naropin, AstraZeneca AB, Sweden) was diluted at room temperature in bath solution to 5 mmol/L as the stocking solution. Different concentrations (10, 50, 100, 300, and 1000 μmol/L) were then applied to the cells by continuous superfusion during the experiments via a fast gravity-driven perfusion system. After 10-min perfusion with the drug, step pulses as illustrated in the figure legends were used to investigate the effect of ropivacaine on rNav1.2 and rNav1.5 subtypes.

2.4 Data analysis For rNav1.2, capacitance currents and leak currents were corrected by subtraction of the currents recorded in the presence of 500 nmol/L tetrodotoxin (TTX). Data were acquired by Cellwork Reader 3.6 (npi instruments, Germany), recorded by Cellwork E 5.5 (npi Instruments, Germany), and analyzed with Origin 8.0 software (OriginLab Corp., Northampton, MA, USA). For rNav1.5, data were analyzed using the Clampfit 8.2 (Axon Instruments, USA) and Origin 8.0 (OriginLab Corp., Northampton, MA, USA).

Data were presented as mean±SEM and analyzed using two sample independent *t*-test. $P < 0.05$ was considered as statistically significant.

The fittings of the dose–response curves were carried out using a Hill's equation: % inhibition=A/[1+(IC_{50}/Ropivacaine)^h]+C, where IC_{50} indicated the half maximal effective concentration and "h" was the Hill coefficient.

Conductance was calculated using the equation: $G(V) = I_{peak}(V)/(V-V_{rev})$, where I_{peak} indicated the peak amplitude of the Na^+ current, while V and V_{rev} represented the test potential and the reverse potential, respectively.

The voltage dependence of steady-state activation was quantified by fitting the conductance measures to a Boltzmann function: $G(V) = G_{max}/[1+\exp(V_{test} - V_{1/2})/K]$.

Steady-state inactivation was fitted to a Boltzmann function with a non-zero pedestal (I_0) calculated as $I/I_{max} = (1 - I_0)/[1+\exp(V_{1/2} - V_{test})/K]+I_0$, where $V_{1/2}$ indicated the test potential at which the channels were half-maximally activated and K was the slope factor.

3 Results

3.1 The peak Na^+ currents of both rNav1.2 and rNav1.5 were inhibited by ropivacaine Ropivacaine induced the dose-dependent inhibition of both rNav1.2α and rNav1.5α peak currents. Fig. 1 showed the representative current traces of rNav1.2 (Fig. 1A) and rNav1.5 (Fig. 1B) before and after ropivacaine superfusion at different concentrations (10, 100, and 300 μmol/L). The resulting dose-response curves (Fig. 1C) showed that the values of Hill coefficients were 4.1 for rNav1.2 and 0.64 for rNav1.5, respectively. For rNav1.2, the IC50 value (the half maximal inhibitory concentration of ropivacaine) was (155±8.3) μmol/L, while for rNav1.5, the IC50 value was (69.8±10.3) μmol/L.

Fig. 2 showed the representative whole-cell Na^+ current traces from oocytes expressing rNav1.2 under control condition (Fig. 2A) and in the presence of 300 μmol/L ropivacaine (Fig. 2B). I_{Na} was elicited by depolarized to -20 mV with 2 Hz from the holding potential of -100 mV. Fig. 2C showed the representative I-V curves of rNav1.2 with or without ropivacaine. The channels were activated at about -40 mV, reaching a peak at -10 mV.

Fig. 3 showed the representative whole-cell Na^+ current traces from HEK293t cells expressing rNav1.5 under control condition (Fig. 3A) and in the presence of 300 μmol/L ropivacaine (Fig. 3B). I_{Na} was evoked using 70 ms test pulses ranged from -100 mV to +40 mV with 10 mV increment at the holding potential of -140 mV. The representative I-V curves of rNav1.5 before and after ropivacaine treatment were shown in Fig. 3C. Before and after perfusion of ropivacaine, rNav1.5 currents were activated at approximately -60 mV and reached a peak at about -20 mV.

3.2 Effects of ropivacaine on the gating properties of rNav1.2 and rNav1.5 The effects of ropivacaine on the steady-state activation of rNav1.2 and rNav1.5 were investigated. The activation curves were derived from I/V curves (see Methods). The half-maximal activation voltage ($V_{1/2}$) and the slope factor (K_v) were fitted according to a Boltzmann function. It was observed that ropivacaine (200 and 300 μmol/L) did not affect the steady-state activation of rNav1.2 or rNav1.5 channel (Fig. 4). There was no significant difference in the half maximal voltage ($V_{1/2}$) and the slope factor (K_v) between control and treatment groups in either sodium channel subtype.

For rNav1.2, a hyperpolarizing shift of the half maximal

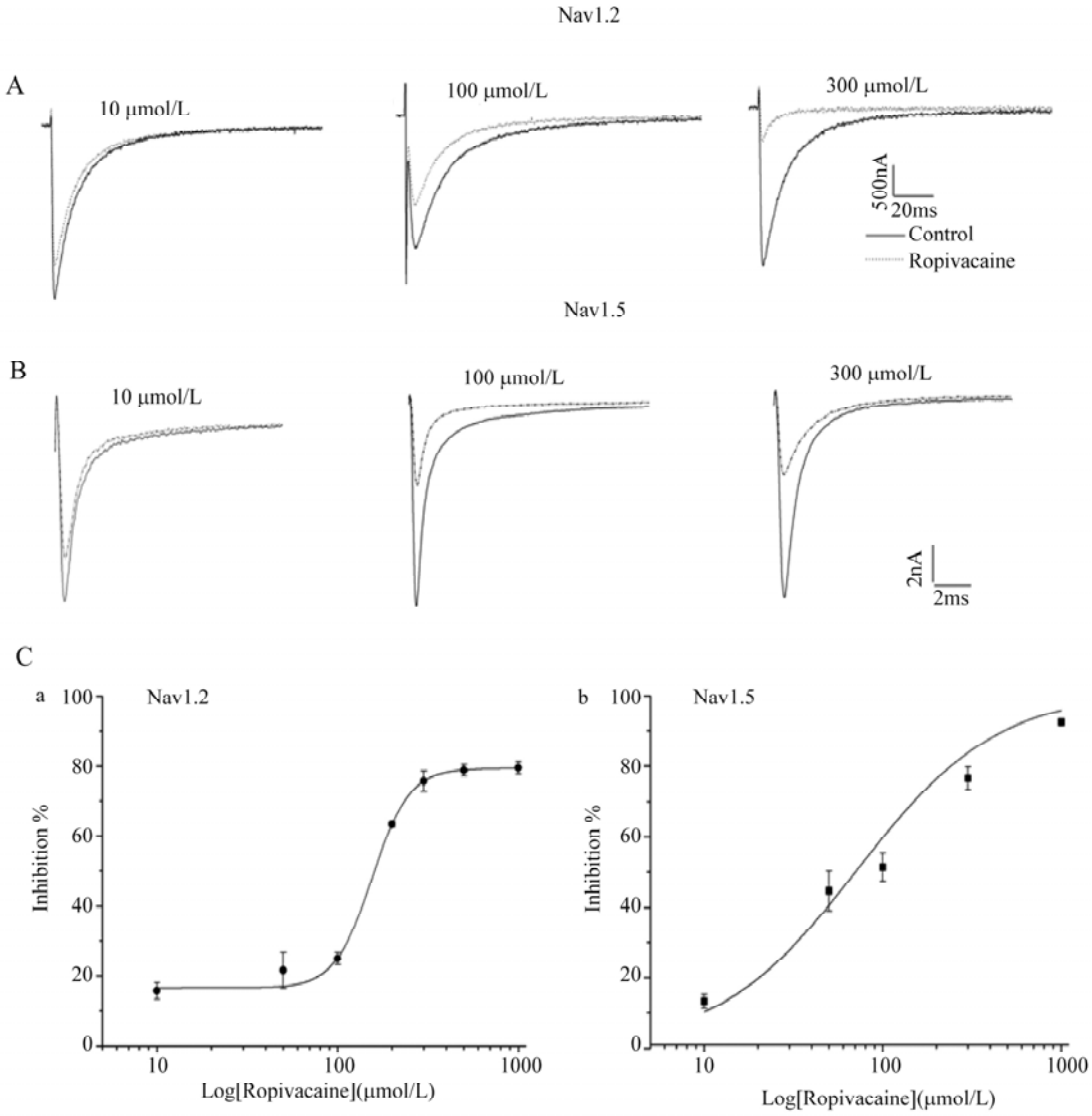

Fig. 1 Dose-dependent blockade of rNav1.2 and rNav1.5 currents by ropivacaine. A: After treatment with ropivacaine at 10, 100, and 300 μmol/L, whole-cell Na^+ currents of rNav1.2 were evoked every 5 s by 200 ms pulses to -10 mV from a holding potential of -100 mV until current was stabilized. B: Whole-cell Na^+ currents of rNav1.5 were evoked every 5 s using 70 ms test pulses ranging from -100 mV to +40 mV with 10 mV increments under a holding potential of -140 mV. C: Dose–response curves for rNav1.2 (a) and rNav1.5 (b) were obtained from fits of a Hill equation.

inactivation voltage ($V_{1/2}$) was observed in the presence of 200 μmol/L ropivacaine. The value of half maximal inactivation voltage was shifted by 10.8 mV, from (-52.83±0.75) mV to (-63.63±0.99) mV (n=6) ($P < 0.05$) and the slope factor was increased by 3.87, from (14.9±0.67) to (18.77±0.97) (Fig. 4A). For rNav1.5, 300 μmol/L ropivacaine significantly shifted the midpoint of the steady-state inactivation curve by 12.1 mV ($P < 0.01$) towards more hyperpolarized values, and the slope factor of the curve was also significantly shifted by 1.95 (Fig. 4B).

3.3 Use-dependent inhibition of both rNav1.2 and rNav1.5 subtypes by ropivacaine The use-dependent inhibition of rNav1.2 and rNav1.5 subtypes was tested by applying a train of 50 short 8-ms depolarizing pulses (-10 mV for rNav1.2 under the holding potential of -100 mV, and -20 mV for rNav1.5 under the holding potential of -140 mV). Dramatic differences

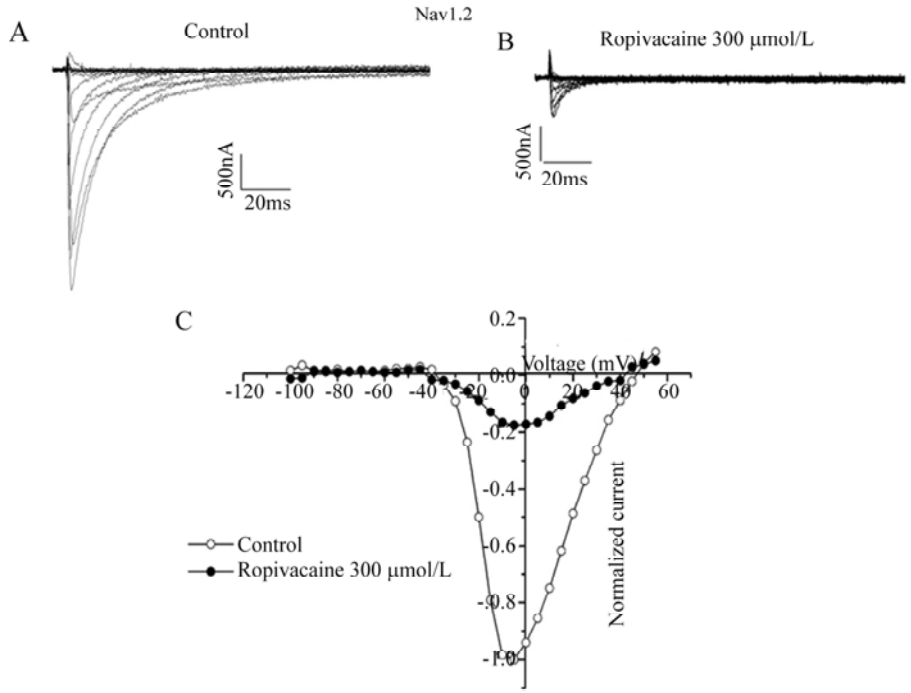

Fig. 2 Whole-cell Na^+ current traces of oocytes expressing rNav1.2 before (A) and after (B) treatment with 300 μmol/L ropivacaine. C: the effects of ropivacaine (300 μmol/L) on the current–voltage relationship (I/V curves).

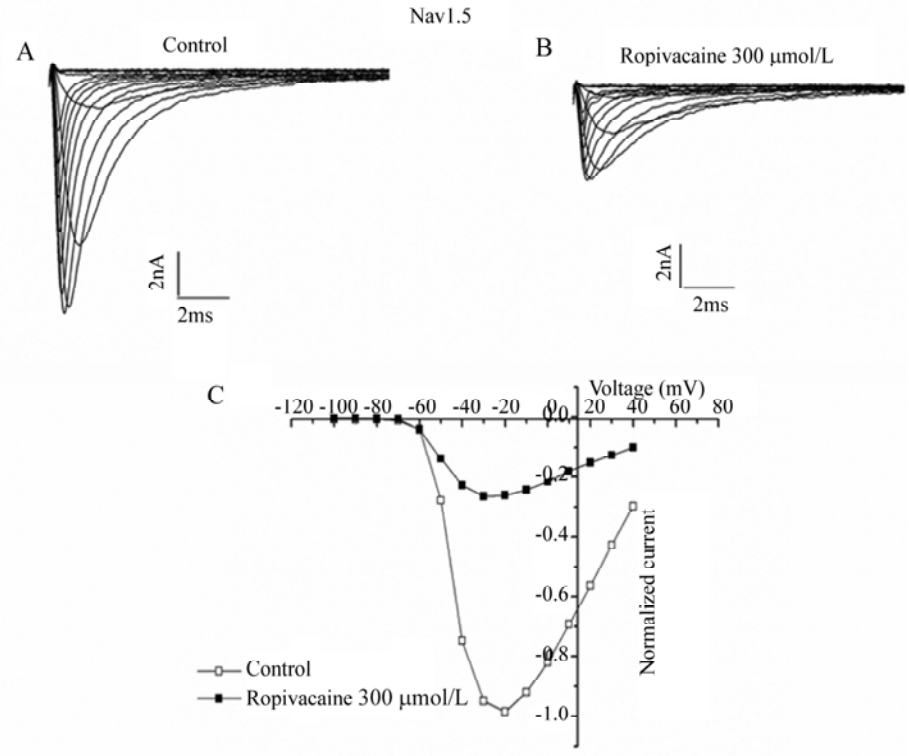

Fig. 3 Whole-cell Na^+ current traces of HEK293t cells expressing rNav1.5 before (A) and after (B) treatment with 300 μmol/L ropivacaine. C: the effects of ropivacaine (300 μmol/L) on the current–voltage relationship (I/V curves).

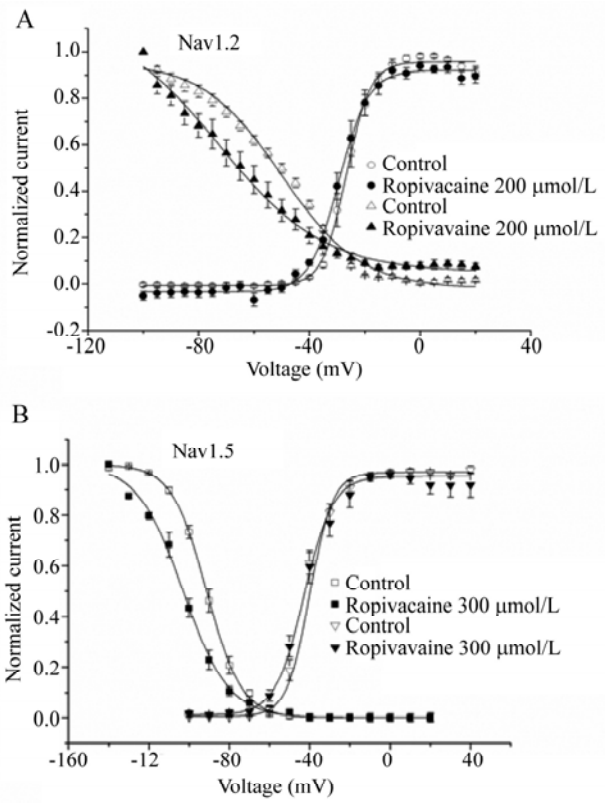

Fig. 4 Effect of ropivacaine on the steady-state activation and steady-state inactivation curves of rNav1.2 (A) and rNav1.5 (B). Steady-state activation curves were derived from the same family of currents used for the I/V curves (Fig. 2C, Fig. 3C) using the standard procedure (see Methods). For rNav1.2, steady-state inactivation was determined using 500 ms conditioning pulses to voltages between -100 mV and +20 mV and a standard test pulse to -10 mV. For rNav1.5, steady-state inactivation were determined using 115 ms conditioning pulses to voltages between -140 mV and +20 mV and a standard test pulse to -20 mV. Test currents were normalized and plotted against the conditioning voltage. The smooth curves were Boltzmann fits (the equations were shown in Methods).

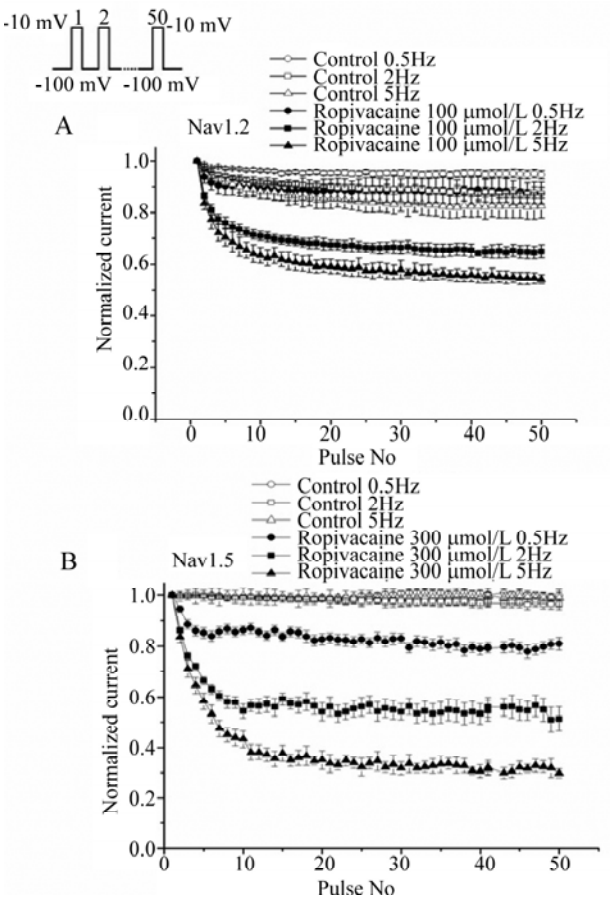

Fig. 5 Frequency-dependent inhibition of rNav1.2 (A) and rNav1.5 (B) currents in the presence or absence of ropivacaine (100 μmol/L for rNav1.2, 300 μmol/L for rNav1.5). A: For rNav1.2, oocyte potentials were held at -100 mV, and a train of fifty 8-ms pulses (-10 mV) was applied at 3 different frequencies (0.5, 2 and 5 Hz), with the interpulse potential set at -100 mV. B: For rNav1.5, HEK293t cell potentials were held at -140 mV, and a train of fifty 8-ms pulses (-20 mV) was applied at 3 different frequencies (0.5, 2 and 5 Hz), with the interpulse potential also set at -140 mV. The peak currents elicited by each pulse were normalized to the current of the first pulse (P*n*-P1, where *n*=1–50) and then plotted against pulse number. The top panel showed a schematic representation of the electrical protocol used.

were observed in the sensitivities of both rNav1.2 and rNav1.5 to ropivacaine among the 3 different frequencies (0.5, 2 and 5 Hz). As shown in Fig. 5A, in the absence of ropivacaine, there was a slight decrease in rNav1.2 channel availability when stimulation was performed at frequencies between 0.5-5 Hz, and the currents remained still above 85% of their initial value. In the presence of 100 μmol/L ropivacaine, rNav1.2 channel availability was reduced to approximately 90%, 70% and 60% of their maximal peak value when stimulated at 0.5, 2 and 5 Hz, respectively. On the other hand, rNav1.5 was more sensitive to the stimulation frequency when superfused with 300 μmol/L ropivacaine (Fig. 5B). rNav1.5 channel availability was reduced to approximately 80%, 50% and 30% of their initial maximal peak when stimulated at 0.5, 2 and 5 Hz, respectively. On the contrary, under control condition, almost no reduction in current was observed when the channel was pulsed at any of the frequencies.

4 Discussion

In the present study, the sensitivities of rNav1.2α (brain

type) and rNav1.5α (cardiac type) to ropivacaine were confirmed, and the pharmacological modulating modes of ropivacaine on both subtypes were characterized. The results showed that ropivacaine could inhibit peak Na^+ currents of Nav1.2 and Nav1.5 channels in a dose-dependent manner as other local anesthetics. However, Nav1.2 and Nav1.5 subtypes exhibited different sensitivities to ropivacaine, since the IC_{50} for Nav1.2 block was 155 μmol/L while that for Nav 1.5 block was 69.8 μmol/L, similar to the finding in DRG neurons where the TTX-R currents are more sensitive to ropivacaine than the TTX-S currents[13]. On the other hand, the IC_{50} values of lidocaine, mexiletine and benzocaine for Nav1.2α have been demonstrated to be 1105 μmol/L, 337 μmol/L and 814 μmol/L, respectively[15]. Therefore, it is obvious that ropivacaine has a higher potency than do the above mentioned local anesthetics.

In addition, ropivacaine had similar effects on the gating properties of Nav1.2 and Nav1.5 channels. Ropivacaine did not shift the steady-state activation curve of Nav1.2 or Nav1.5. In contrast, it shifted the steady-state inactivation curves of Nav1.2 and Nav1.5 toward more hyperpolarized values by 10.8 mV and 11.2 mV, respectively. The above observation strongly indicates that the blocking mechanism of ropivacaine on Na^+ channels is similar to that of other local anesthetics such as lidocaine and benzocaine[15], mainly by altering the steady-state inactivation, but not the steady-state activation of Na^+ channels.

During depolarization, the conformation of Na^+ channels undergoes a series of changes: "the resting state", "the closed state", "the open, ion-conducting state" and "the inactivated state". Nearly full-sized Na^+ currents could be elicited during the first depolarizing impulse in the presence of a local anesthetic, but subsequent impulses elicit gradually smaller peak currents. When Na^+ channels are subject to a train of depolarizing pulses, the number of channels available to open is reduced and they progressively accumulate in the inactivated state. This accumulation of inhibition has been termed "use-dependent block" [7,16]. In this study, we found that repetitive pulses caused a large current reduction for Nav1.2 but had little effect on Nav1.5. Ropivacain induced a great decrease in Na^+ currents for both channels following high-frequency stimulation, suggesting that the drug preferentially binds to inactivated channels.

In conclusion, the present study demonstrates that ropivacaine has different effects on brain and heart subtypes of sodium channels, and it preferentially blocks Nav1.5 channels. As ropivacaine could potentially induce central nervous system and cardiovascular toxicity at high plasma concentrations, the results would be helpful in further understanding clinical toxicology and pharmacology of ropivacaine.

Acknowledgements: This work was supported by the National Basic Research Development Program of China (No. 2006CB500801, 2010CB529806), the National Natural Science Foundation of China (No.30900422), the Natural Science Foundation of Shanghai Municipality, China (No.08JC1409500), State Key Laboratory of Medical Neurobiology, Fudan University (No.09-02), and National Laboratory of Biomacromolecules, Institute of Biophysics, Chinese Academy of Sciences (No.O5SY021097).

References:

[1] Brockway MS, Bannister J, McClure JH, McKeown D, Wildsmith JA. Comparison of extradural ropivacaine and bupivacaine. Br J Anaesth 1991, 66(1): 31-37.

[2] Zaric D, Axelsson K, Philipson L, Nydahl PA, Larsson P, Jansson JR, *et al*. Blockade of the abdominal muscles measured by EMG during lumbar epidural analgesia with ropivacaine—a double-blind study. Acta Anaesthesiol Scand 1993, 37(3): 274-280.

[3] Kopacz DJ, Emanuelsson BM, Thompson GE, Carpenter RL, Stephenson CA. Pharmacokinetics of ropivacaine and bupivacaine for bilateral intercostal blockade in healthy male volunteers. Anesthesiology 1994, 81(5): 1139-1148.

[4] Guo XT, Castle NA, Chernoff DM, Strichartz GR. Comparative inhibition of voltage-gated cation channels by local anesthetics. Ann N Y Acad Sci 1991, 625: 181-199.

[5] Scholz A. Mechanisms of (local) anaesthetics on voltage-gated sodium and other ion channels. Br J Anaesth 2002, 89(1): 52-61.

[6] Delgado JN, Remers WA. Textbook of Organic Medicinal and Pharmaceutical Chemistry. Philadelphia: Lippincott-Raven Publishers, New York, 1998: 631-655.

[7] Courtney KR. Mechanism of frequency-dependent inhibition of

sodium currents in frog myelinated nerve by the lidocaine derivative GEA. J Pharmacol Exp Ther 1975, 195(2): 225-236.
[8] Yu FH, Westenbroek RE, Silos-Santiago I, McCormick KA, Lawson D, Ge P, *et al*. Sodium channel beta4, a new disulfide-linked auxiliary subunit with similarity to beta2. J Neurosci 2003, 23 (20): 7577-7585.
[9] Goldin AL, Barchi RL, Caldwell JH, Hofmann F, Howe JR, Hunter JC, *et al*. Nomenclature of voltage-gated sodium channels. Neuron 2000, 28(2): 365-368.
[10] Goldin AL. Evolution of voltage-gated Na^+ channels. J Exp Biol 2002, 205(Pt 5): 575-584.
[11] Gong B, Rhodes KJ, Bekele-Arcuri Z, Trimmer JS. Type I and type II Na^+ channel alpha-subunit polypeptides exhibit distinct spatial and temporal patterning, and association with auxiliary subunits in rat brain. J Comp Neurol 1999, 412(2): 342-352.
[12] Kallen RG, Sheng ZH, Yang J, Chen LQ, Rogart RB, Barchi RL. Primary structure and expression of a sodium channel characteristic of denervated and immature rat skeletal muscle. Neuron 1990, 4(2): 233-242.
[13] Oda A, Ohashi H, Komori S, Iida H, Dohi S. Characteristics of ropivacaine block of Na^+ channels in rat dorsal root ganglion neurons. Anesth Analg 2000, 91(5): 1213-1220.
[14] Ding, HL, Zeng YM, Li XD, Jiang WP, Duan SM. Effects of ropivacaine on sodium, calcium, and potassium currents in guinea pig ventricular myocytes. Acta Pharmacol Sin 2002, 23(1): 50-54.
[15] Weiser T. Comparison of the effects of four Na^+ channel analgesics on TTX-resistant Na^+ currents in rat sensory neurons and recombinant Nav1.2 channels. Neurosci Lett 2006, 395(3):. 179-184.
[16] Ulbricht W. Kinetics of drug action and equilibrium results at the node of Ranvier. Physiol Rev 1981, 61(4): 785-828.

罗哌卡因对脑型和心肌型电压门控钠通道亚型失活的选择性调制

程慧雯，杨宏天，周京晶，吉永华，朱红艳
上海大学神经药理与毒理实验室，上海 200444

摘要：目的 本研究旨在探讨酰胺类局部麻醉药罗哌卡因对外源表达的大鼠脑型(rNav1.2)和心肌型(rNav1.5)电压门控钠通道电流的药理调制作用。**方法** 运用双电极和膜片钳全细胞记录技术记录全细胞电流。**结果** 罗哌卡因能以浓度和频率依赖的方式抑制rNav1.2和rNav1.5亚型通道的峰钠电流，其中Nav1.5亚型通道对罗哌卡因的敏感性相对较高。此外，罗哌卡因能使 rNav1.2 和 rNav1.5 亚型通道的稳态失活曲线向超极化方向显著偏移，但对激活曲线没有影响。通过重复高频去极化刺激，罗哌卡因能以使用依赖性的方式抑制 rNav1.2 和 rNav1.5 亚型通道的电流。**结论** 结果提示罗哌卡因的药理机制体现在对钠通道亚型失活态的调制上。该结果有助于进一步理解罗哌卡因对脑型和心肌型电压门控钠通道的药理调制作用。

关键词： 罗哌卡因；局部麻醉药；电压门控钠通道亚型的敏感性；电生理记录